International Journal of Hydrogen Energy 63 (2024) 609–617

Contents lists available at ScienceDirect

International Journal of Hydrogen Energy

journal homepage: www.elsevier.com/locate/he

New laminar flame speed correlation for lean mixtures of hydrogen combustion with water addition under high pressure conditions

D.N. Rrustemi, L.C. Ganippa, T. Megaritis, C.J. Axon *

Department of Mechanical and Aerospace Engineering, Brunel University London, Uxbridge, London, UB8 3PH, UK

ARTICLE INFO

Handling Editor: Dr M Mahdi Najafpour

Keywords:
Flame speed correlation
Hydrogen
ICE
Laminar flame speed
Steam dilution

ABSTRACT

Hydrogen may become a substitute for liquid fossil fuels, contributing to greenhouse gas emissions reductions in internal combustion engines. Numerical simulations play a critical role in the advancement of these engines, with laminar flame speed being the main input. Experimental data of hydrogen flame speed at elevated pressures are scarce, due to the instability of the flames. Nonetheless, stable hydrogen flames can be predicted using chemical kinetics models. Moreover, the injection of water into the hydrogen fuelled engine could offer several benefits to engine combustion and emission performance, as it modulates the laminar flame speed within the combustion chamber and this effect has not been completely understood. Currently, no correlation exists to predict the laminar flame speed of hydrogen-air combustion with water addition under lean mixture engine operating conditions. In this study, we have extended the newly developed laminar flame speed correlation of hydrogen-air combustion to account for the effects of water addition under engine relevant conditions by using chemical kinetic laminar flame speed values. The laminar flame speed correlation was derived for pressures from 10 to 70 bar, temperatures from 400 to 800 K, equivalence ratios from 0.35 to 1 and water addition by mole from 0 to 20%. The hydrogen laminar flame speed correlation was expressed using polynomial forms with reduced order and number of terms with optimized values of coefficients. Additionally, a new exponential term was proposed to the power term α of the laminar flame speed correlation to capture the coupled effects of pressure and temperature on laminar flame speeds under engine-relevant lean burn water-diluted operating conditions.

1. Introduction

Limited fossil fuel reserves and environmental constraints are incentivising exploration of alternatives for carbon-free fuels for use in internal combustion engines [1]. Hydrogen has advantageous properties as a carbon-free fuel [2,3] because its thermochemical properties differ significantly compared to traditional fuels such as gasoline, diesel, and methane [4]. A notable difference is the laminar flame speed (LFS), one of the most important inputs in all numerical combustion models, an essential tool for improving spark ignition (SI) engines. The LFS is used to assess the stability of flames and to characterize the transition between deflagration and detonation [5], and crucial for turbulent flame calculations. Generating hydrogen LFS data from experiments or chemical kinetic simulations across a wide range of operating conditions is time-consuming, therefore, laminar flame speed correlations could provide reliable values. Experimental data for hydrogen combustion at the elevated pressures of engine-relevant conditions are scarce, as the flames are unstable [6]. However, stable hydrogen flames could be predicted by using chemical kinetics models [7], once the kinetic mechanism is validated. Most of the available LFS correlations are fitted using a power law [8] where the influence of equivalence ratio, pressure and temperature are independent as shown in Eq. (1),

$$S_l(\varnothing, P, T_u) = S_{l0}\left(\frac{T_u}{T_0}\right)^{\alpha}\left(\frac{P}{P_0}\right)^{\beta} \quad (1)$$

The laminar flame speed S_l is a function of equivalence ratio $\varnothing$, unburned gas temperature T_u, and pressure P at a reference pressure P_0 and temperature T_0. The terms S_{l0} , α and β represent the flame speed at a reference condition, temperature and pressure power coefficients, respectively. Power coefficients α and β differ for each fuel and can be determined from experimental or numerical approaches [9]. Most correlations [7,10] only express the power coefficients α and β as dependent on the equivalence ratio. However, numerous experimental studies have shown that the coefficient β varies with both pressure and equivalence ratio [5,9,11]. Additionally, Verhelst et al. [6] demonstrated a strong

* Corresponding author.
E-mail addresses: Dardan.Rrustemi@brunel.ac.uk (D.N. Rrustemi), Lionel.Ganippa@brunel.ac.uk (L.C. Ganippa), Thanos.Megaritis@brunel.ac.uk (T. Megaritis), Colin.Axon@brunel.ac.uk (C.J. Axon).

https://doi.org/10.1016/j.ijhydene.2024.03.177
Received 26 January 2024; Received in revised form 4 March 2024; Accepted 13 March 2024
Available online 21 March 2024

Nomenclature

Symbols

S_l	laminar flame speed (m/s)
$\varnothing$	equivalence ratio
P	pressure (bar)
T	temperature (K)
f	residual gas fraction
α	temperature power coefficient
β	pressure power coefficient
χ	water molar fraction

Acronyms

NOx	oxides of nitrogen
LFS	laminar flame speed
SI	spark ignition

Subscripts

0	reference condition
U	unburned

relationship between the effects of pressure and equivalence ratio on the hydrogen LFS. To account for the observed nonlinear effects of the pressure on the hydrogen LFS [6] integrated the coupled effects of the equivalence ratio and pressure to calculate the reference flame speed S_{l0} and pressure exponent β. Moreover, [12] showed that for the gasoline LFS correlation the power law formulation of [8] was unable to capture the non-power behaviours. The observed coupling of temperature-pressure dependence on the LFS, was resolved by incorporating a logarithmic dependence of the flame speed on the temperature and pressure terms. Additionally, for the methane LFS fitting [11], proposed to modify the power-law of [8] by incorporating the pressure effect on the temperature power coefficient and by incorporating the temperature effect into the pressure power coefficient at various equivalence ratios, to study the effect of pressure and temperature on the methane LFS. The same fitting method for methane LFS fitting was also documented in Ref. [5]. Whereas, in Ref. [13], a temperature scaling factor at various equivalence ratios was introduced to fit the LFS of the gasoline surrogate, the same approach was also used in Ref. [14] for the fitting of the LFS for various sets of toluene reference fuels. Moreover, several machine learning procedures for LFS could be found in Refs. [15–18]. In this study, the hydrogen LFS is correlated using the power law of [8] and the effects of the equivalence ratio and pressure coupled to calculate the reference flame speed S_{l0} and pressure exponent β proposed by Ref. [6]. The temperature-power coefficient α is modelled as a function of pressure and temperature, and an additional exponential temperature term is proposed to capture coupled temperature-pressure effects on the hydrogen LFS. The leading automobile manufacturers are developing boosted and downsized hydrogen SI engines to compete with current gasoline engines. Boosting provides higher thermal efficiencies, but makes the engine prone to combustion abnormalities such as knocking [19]. It was shown [20] that low-temperature combustion methods (introduction of a cooled exhaust gas recirculation, lean burn operation or water injection) are effective on mitigating knock on hydrogen fuelled SI engines. The injection of water into the cylinder could offer significant benefits for the combustion process and engine emissions [20,21]. The addition of water in hydrogen-air combustion has three main effects on flame speed: 1) the dilution effect, which reduces the net reaction rate, 2) the thermal-diffusion effect, which alters the thermodynamic and transport properties of the reactants, and 3) the chemical effect, which occurs due to the participation of the diluent in elementary kinetic reactions [22]. The chemical effect due to adding water to the hydrogen-air reactive mixture alters the reaction mechanisms, not only by the presence of water in the elementary reactions, but the presence of water vapour can facilitate the third-body stabilisation reactions [23]. It is important to note that hydrogen/air flames, with or without water dilution, will not be stable in any combustion application due to factors such as: Darrieus-Landau, Rayleigh-Taylor, heat transfer from the flame front into the unburned mixtures and variations in thermal and mass-diffusivities [24]. These flame front instabilities will cause the flame growth relative to its characterized LFS and result in cellular structure, which are more prone to occur under lean-mixture and high-pressure hydrogen combustion engine environment [25]. Also, the flame thickness is an important parameter to be considered while studying turbulent combustion in internal combustion engines [26] but this work is focused only on the development of a LFS correlation based on chemical kinetics for hydrogen combustion with water addition at engine relevant conditions. The proposed correlation for hydrogen LFS with water addition could be relevant in assessing the impact of the instabilities of the experimental data under engine relevant conditions. It could also be used for modelling the turbulent burning velocities due to the scarcity of hydrogen LFS data at elevated pressures and temperatures. This study can be divided into two parts (1) pure hydrogen LFS correlation, and (2) water-diluted hydrogen LFS correlation.

2. Methodology

The freely propagating hydrogen flames, with and without water addition, were simulated in the CONVERGE solver [27]. Concurrently, polynomial expressions of reduced order were developed with optimized values of coefficients to predict the LFS for hydrogen combustion under lean mixture operation at engine-relevant lean-burn water-diluted operating conditions.

2.1. Numerical model

The chemical kinetic model of a freely propagating hydrogen flame consisting of 19 elementary reversible reaction mechanisms that was developed by Li et al. [28] was used to calculate the LFS of hydrogen-air combustion under various pressures ranging from 10 bar to 70 bar, temperatures ranging from 400 to 800 K, equivalence ratios ranging from 0.35 to 1, and for 0–20% molar fraction of water. More than 5000 LFS values were calculated through CONVERGE [27] using a chemical kinetic model [28] in a well-stirred reactor for the selected range of conditions. These data were used to develop a new correlation capable of predicting the LFS of hydrogen-air combustion with water addition in any practical power generation device.

The chemical kinetic model [28] has already been validated against the published experimental LFS of hydrogen-air combustion for temperatures ranging from 298 to 3000 K, pressures from 0.3 to 87 atm, and equivalence ratios from 0.25 to 5. The experimentally measured values of the LFS were obtained either through the burner flame stabilisation [29,30] or spherical flame propagation in a chamber [31,32]. The main difference is that the burner flames did not consider the stretch rate effect, hence the experimental data obtained through this method was greater than the experimental values obtained through spherical flame propagation method, where the flame propagation was corrected based on flame stretch rate. A comparison of published [29–32] experimental results of hydrogen burning speeds with the calculated LFS from the chemical kinetics model at different equivalence ratios [28] are shown in Fig. 1. The simulated values of LFS show good agreement with the experimentally measured stretch-free burning velocities of [31,32] under lean operating regions of $\Phi < 1$.

The comparison of published experimental data [33,34] with simulations performed under 1 atmospheric pressure and at a temperature of 373 K, with varied equivalence ratios of the hydrogen-air mixture from 0.5 to 1.7 for steam dilutions at 12% and 22% by volume, are shown in Fig. 2. It can be observed that both the experimental and simulated LFS

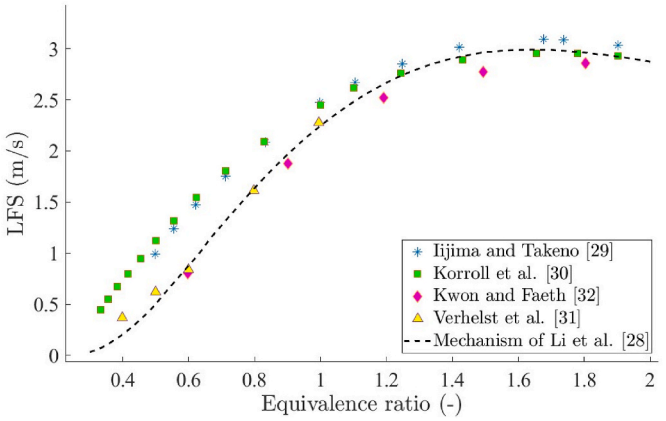

Fig. 1. Laminar burning velocities at different equivalence ratios at P of 1 atm and T of 300 K. The markers represent the experimental data values [29–32]. The dashed line represents the hydrogen LFS calculated from the detailed chemical kinetics with mechanism of [28].

exhibit the similar global trend with varying equivalence ratios. The simulated LFS results were within a maximum of an 11% error margin when compared to the experimental data of [33], and within a maximum error margin of 6% for the experimental data of [34]. The data presented in Figs. 1 and 2 show that the hydrogen kinetic mechanism [28] is in good agreement with the experimental data of [31,32] for neat hydrogen-air lean mixture combustion, as well as for water addition under lean hydrogen combustion [33,34]. Therefore, the chemical kinetic model of [28] was used in this work as the basis to calculate the lean-burn water-diluted hydrogen LFS values under high pressure engine-relevant operating conditions.

2.2. Laminar flame speed correlation

Generation of LFS data from chemical kinetic models for varying operating condition are time consuming. Therefore it is useful to develop a correlation for hydrogen that can predict the LFS under complex engine operating conditions with high degree of accuracy, particularly for water injection strategies favouring NOx reduction [20]. The formulation of [6] in Eq. (2) was used to fit the hydrogen with water addition LFS,

$$S_l(\varnothing, P, T_u, \chi) = S_{l0}(\varnothing, P, T_u)\left(\frac{T_u}{T_0}\right)^{\alpha(\varnothing,P,T_u)}(1 - \chi * F(\varnothing, P, T_u, \chi)) \quad (2)$$

The parameters S_{l0}, α and F were fitted using polynomials of least order ($R^2 = 0.99$). A reference pressure ($P_0 = 5$ bar) and a reference temperature ($T_0 = 600$ K) were set to make the pressure and temperature non-dimensional. Initially just over 2500 LFS data were fitted using the Levenberg-Marquardt algorithm [12] for S_{l0} (Eq. (2)) at various pressures and equivalence ratios at a fixed temperature of 600 K. The correlation was tested to ensure that no spurious values were generated, confirmed by conducting a non-negative constrained multivariate regression analysis. The Akaike Information Criterion (AIC) [35] was adopted to explore different combinations of the predictors to determine the most optimized fitting model (Eq. (3)), the corresponding fittings coefficients a_i are shown in Table 1.

$$\begin{aligned} S_{l0} = {} & a_1\varnothing^2 + a_2\varnothing^3 + a_3\log(\varnothing) + a_4\log\left(\frac{P}{P_0}\right) + a_5\, exp(-\varnothing) \\ & + a_6\,\varnothing\, log\left(\frac{P}{P_0}\right) + a_7\, log(\varnothing)\left(\frac{P}{P_0}\right) + a_8\exp(-\varnothing)\left(\frac{P}{P_0}\right) \end{aligned} \quad (3)$$

Table 1
Coefficients a_i to be used in Eq. (3), coefficients b_i to be used in Eq. (4), coefficients c_i to be used in Eq. (5) and coefficients d_i to be used in Eq. (6), for conditions of $P_0 = 5$ bar and $T_0 = 600$ K.

a_i	Value	b_i	Value	c_i	Value	d_i	Value
a_1	13.7528	b_1	−1.2354	c_1	9.294	d_1	4.9667
a_2	−4.3159	b_2	3.45 e−05	c_2	−27.6	d_2	−3.0818
a_3	−1.2832	b_3	0.10518	c_3	30.70	d_3	0.4600
a_4	1.0261	b_4	−0.5332	c_4	−14.76	d_4	−0.2508
a_5	−3.4574	b_5	4.3181	c_5	2.853	d_5	0.4331
a_6	−3.7039	b_6	1.8539			d_6	3.2483
a_7	0.1490	b_7	−0.5166			d_7	−3.0087
a_8	0.2545	b_8	−0.6528			d_8	−8.5907
		b_9	3.2115			d_9	0.1448

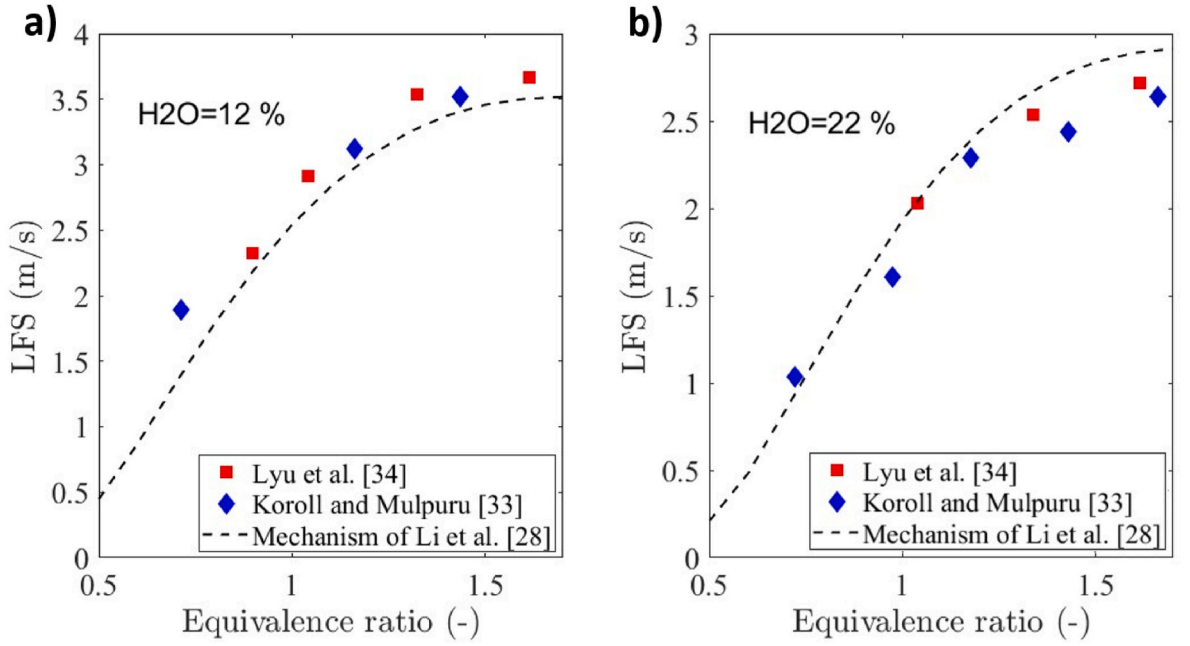

Fig. 2. Laminar flame speed of hydrogen with 12% and 22% water addition at various equivalence ratios (P = 1 atm, T = 373 K). The dashed line is the simulated laminar flame speed using mechanism of [28], and the markers represent experimental data [33,34].

Fig. 3 shows the comparison of calculated initial S_{l0} values obtained from the chemical kinetics model [28] with the newly developed correlation (Eq. (3)). It can be seen that the correlation predicted S_{l0} with good accuracy, where 98% of data fitted well within 10% error. However, it can be seen from the inset plot in Fig. 3 that the values for the LFS lower than 0.3 m/s did not fit within the 10% error margin. This was due to the weighting factor, which could not be increased further since it tended to reduce the correlation accuracy for the entire operating condition range.

To explore the dependence of pressure, temperature and equivalence ratio on the exponent term α a polynomial was developed for $\alpha\ (P, \varnothing, T)$ by fitting it with a set of 2000 hydrogen LFS data generated at different conditions. Most of the available LFS correlations [7,10] considered the exponent α only to be dependent on equivalence ratio. Fig. 4 shows the power coefficient α calculated from Eq. (2) once the S_{l0} was known from Eq. (3). It can be seen that the α is not only dependent on $\varnothing$ but also influenced by pressure and temperature, all three parameters are intercoupled. Due to power coefficient α being completely dependent on pressure, temperature and equivalence ratio, α in Eq. (2) has been expressed to account for the effects of pressure and equivalence ratio. Then the temperature effect on the hydrogen laminar flame speed was accounted through the inclusion of an exponential term that relates to temperature and equivalence ratio through the exponent β which is considered to be solely dependent on the equivalence ratio. This third order polynomial of α consisting of 9 coefficients b_i was fitted (R^2 = 0.99). The attained polynomial expression for α is shown in Eq. (4), and the fitting coefficients for b_i are presented in Table 1.

$$\alpha = \left(b_1\varnothing^3 + b_2\left(\frac{P}{P_0}\right)^3 + b_3\varnothing^3\left(\frac{P}{P_0}\right) + b_4\, log\left(\frac{P}{P_0}\right) + b_5\exp(-\varnothing) + b_6\varnothing\, log\left(\frac{P}{P_0}\right) + b_7\log(\varnothing)\left(\frac{P}{P_0}\right) + b_8\exp(-\varnothing)\left(\frac{P}{P_0}\right) + b_9\varnothing\, exp\left(-\frac{P}{P_0}\right)\right) exp\left(\beta\frac{T}{T_0}\right) \quad (4)$$

Where β is dependent only on the equivalence ratio, and it is given in the form as shown in Eq. (5).

$$\beta = c_1\varnothing^4 + c_2\varnothing^3 + c_3\varnothing^2 + c_4\varnothing + c_5 \quad (5)$$

The accuracy of the α term in Eq. (3) due to the inclusion of temperature effect on the hydrogen-air laminar flame speed was compared with the chemical kinetic model [28] for 3000 data points (Fig. 5). The improvement in the accuracy for the hydrogen-air flames through the incorporation of the term $\exp(\beta T/T_0)$ in α as shown in Eq. (4) (black markers), compared with the fitting accuracy without the proposed term $\exp(\beta T/T_0)$ (red markers). It can be observed from Fig. 5 that the accuracy improved significantly for LFS values greater than 3 m/s by incorporating the term, accounting for the temperature-pressure coupling effects. Moreover, it can be seen that for the LFS correlation with the incorporation of the term $\exp(\beta T/T_0)$ in α, most of the data points are within a ±10% accuracy margin, except for few data points at lower values. The prediction accuracy could be improved by improving the accuracy of the chemical kinetics model.

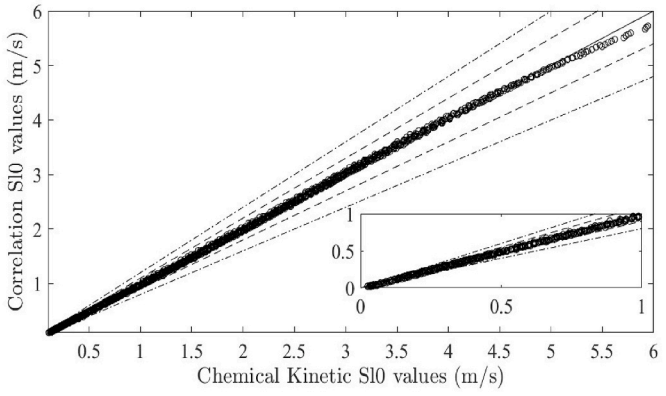

Fig. 3. Chemical kinetic values of S_{l0} compared to correlation S_{l0} values using Eq. (3) with lines of 10% and 20% deviation (P = 10–70 bar, ∅ = 0.35–1, T = 600 K and χ = 0).

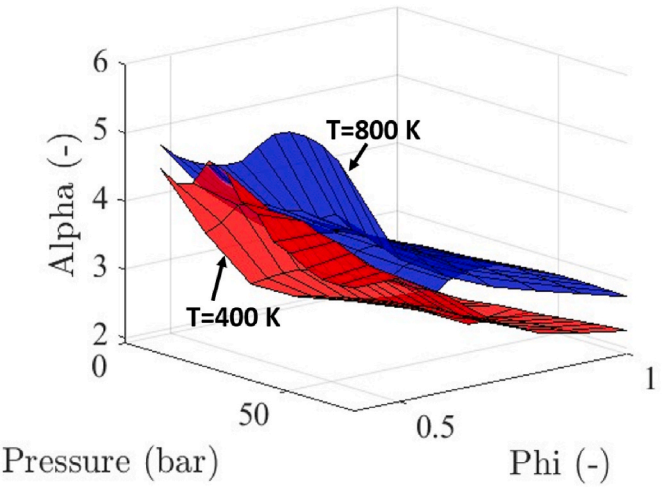

Fig. 4. Alpha at various equivalence ratios and pressures for temperatures of 400 and 800 K for hydrogen.

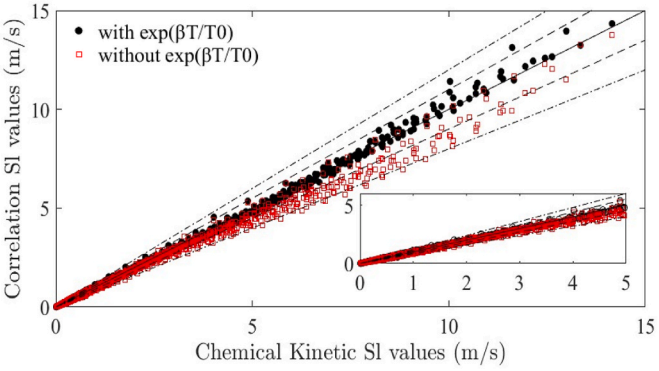

Fig. 5. Chemical kinetic values of laminar flame speed compared to correlation laminar flame speed values with 10% and 20% deviation lines (black markers show laminar flame speed values by calculating α as shown in Eq. (4) and the red makers are the laminar flame speed values without using term). (For interpretation of the references to colour in this figure legend, the reader is referred to the Web version of this article.)

2.3. Laminar flame speed correlation with water addition

The benefits of injecting water into the intake manifold of the hydrogen-fuelled engine [21], are the modulation of the LFS and the local equivalence ratio within the combustion chamber. However, this effect is not fully understood, and no correlation exists to predict the LFS of hydrogen-air combustion with water addition under lean mixture engine operating conditions. We extend the proposed LFS correlation of hydrogen-air combustion (Eq. (2) and (4)) to include the effects of molar fraction of the water on hydrogen combustion under engine-relevant conditions. It has been shown in Ref. [6] that the residual volume fraction term F in the hydrogen flame speed correlation strongly convolves the effects of pressure and equivalence ratio in the correction term. In this work the water addition was incorporated into the flame speed correlation by including the molar fraction of water χ in the term F

in Eq. (2). Note that, the equivalence ratios used in this study only considered fuel and air, and not the global equivalence ratio that is affected by the dilution of the reactive mixture by water vapour. The term F was fitted dependently of pressure, temperature, equivalence ratio and water addition (Eq. (6)) and the coefficients d_i are shown in Table 1. The comparison of values obtained from the correlation and the chemical kinetic model of hydrogen at different pressures, temperatures, equivalence ratios at water addition ranging from 0 to 20% of molar fraction is shown in Fig. 6. About 84% of data fitted within 10% and around 97% of data fitted within the 20% error margin. These data points correspond to the operating conditions used in this study.

$$F = d_1 + d_2\left(\frac{P}{P_0}\right)\chi^2 + d_3\log\left(\frac{P}{P_0}\right) + d_4\left(\frac{P}{P_0}\right)^2\chi^2 + d_5\left(\frac{T}{T_0}\right)^2 + d_6\left(\frac{P}{P_0}\right)\left(\frac{T}{T_0}\right)\chi^2 + d_7\varnothing\left(\frac{T}{T_0}\right) + d_8\chi^2\left(\frac{T}{T_0}\right) + d_9\varnothing^2\left(\frac{P}{P_0}\right) \quad (6)$$

3. Results and discussion

The outcomes of the proposed hydrogen LFS correlation, with and without water addition, are compared to the simulated LFS values at engine-relevant operating conditions. Additionally, the effect of water on hydrogen LFS at elevated pressures are discussed. Finally, to assess the accuracy of the LFS correlation, residual analysis was conducted.

3.1. Comparison of correlation prediction with chemical kinetic values

Fig. 7 shows the hydrogen LFS values obtained from the proposed correlation, and compared with the calculated chemical kinetic flame speed values. This comparison was made for equivalence ratios ranging from 0.35 to 1 with 0–20% (at 5% increment) of water addition, whilst the whole mixture was maintained at a pressure of 30 and 50 bar, and at a temperature between 400 and 800 K. It was observed that the correlation was accurate for all cases (Fig. 7(a–c) and 7(e-h)) except for 20% water addition. In the 20% water addition case, particularly for equivalence rations greater than 0.8 and at a pressure of 30 bar and temperature of 400 K (Fig. 7(h)), the correlation was underpredicting the LFS values. For pressures of 30 bar and 50 bar, a temperature of 600 K, and water addition of 20% at equivalence ratios less than 0.7, the correlation slightly overpredicted the LFS values with the largest deviation being within 13% and 18%, respectively, (Fig. 7(d)). Fig. 7(a–d) also reveal that the LFS predicted by the correlation decreased with an increase in water addition from 0 to 20%. The pure hydrogen LFS decreased by 67% and 72% for 20% water addition at 30 and 50 bar, respectively. For a pressure of 30 bar at ambient reactive mixture temperatures of 400 K and 800 K, the LFS decreased by 60% and 74%, respectively. We observe from Fig. 7(a–d) that by increasing the pressure from 10 to 30 bar, the LFS decreased by 27, 29, 32 and 35% for water addition of 0, 5, 10 and 20%, respectively. Whereas, when the temperature was increased from 400 to 800 K (Fig. 7(e–h)) the LFS increased significantly by 313, 467, 525 and 685% for water addition of 0, 5, 10 and 20%, respectively. It is clear that the new proposed correlation preserves the global trend of the chemical kinetic LFS values at all operating conditions presented in Fig. 7.

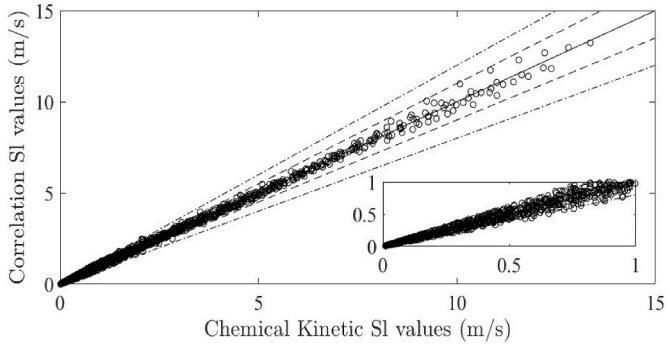

Fig. 6. Chemical kinetic values of laminar flame speed compared to correlation values with 10 and 20% deviation with exp $(\beta T/T_0)$ term (χ = 0–20%, P = 10–70 bar, T = 400–800K, $\varnothing$ = 0.35–1).

3.2. Hydrogen LFS at engine-relevant conditions

Fig. 8 shows the effect of water addition on the hydrogen LFS correlation at various pressures and equivalence ratios and it can be seen that the LFS reduces with increasing pressure. This is in agreement with previous work [36] where it was shown that at water addition of less than 20% by mole fraction, the LFS of hydrogen initially increased and then decreased with increasing pressure. The inflection point occurred at a pressure of 10 atm. Since this study focuses on engine-relevant higher-pressure operating conditions; pressures less than 10 bar were not simulated, hence only a monotonic reduction of the LFS with an increase in pressure was observed. The observed monotonic reduction in flame speeds with pressure could be associated with the reaction order n being less than two due to steam being considered as a third-body in the reaction, hence $S_L \sim P^{n/2-1}$ causes the flame speed to reduce with higher pressures as discussed in Ref. [37]. For neat hydrogen, the LFS decreased by 73%, 66%, and 58% when the pressure was varied from 10 to 70 bar for equivalence ratios of 0.6, 0.8, and 1, respectively (Fig. 8 (a – c)). The proposed correlation and its analysis revealed that pressure has a more pronounced effect on LFS for leaner hydrogen mixtures due to relatively lower energy content in the reactive mixture, which was insufficient to counteract the effect of increased pressure. It is interesting to note that for higher percentages of water addition, specifically at 20% by mole, the LFS was not significantly affected by pressure at levels above 40 bar for mixtures leaner than 0.8 (Fig. 8(a and b)). This phenomenon occurs due to the reduction in global temperature resulting from increased dilution and higher heat capacity of the charge, hence the dissociation reactions were not initiated under higher percentages of water addition. It has been shown experimentally [34] that water addition controls the reaction which causes deflagration of the hydrogen flame at various equivalence ratios, as well as slowing the rise in pressure. The proposed correlation predicts this behaviour (Fig. 8) under all pressures and equivalence ratios, due to an increase in heat capacity of the mixture caused by steam dilution [38]. The equivalence ratio effect on the LFS was consistently seen in all of the presented data. Under leaner mixture conditions for both with and without water addition, an increase in the equivalence ratio caused the LFS to increase (Fig. 8 (a – c)). For the case of pure hydrogen at a pressure of 30 bar and temperature of 700 K, the hydrogen LFS increased by 94 and 201% when the equivalence ratio was raised from 0.6 to 0.8 and 1, respectively. Whereas for water addition of 20% at the same conditions the LFS increased by 179 and 457% when the equivalence ratio was raised from 0.6 to 0.8 and 1, respectively. Though the LFS increases significantly with an increase in equivalence ratio for 20% water addition relative to neat hydrogen combustion, on an absolute scale the magnitude of the hydrogen LFS with water addition is much lower than neat hydrogen combustion. Additionally, the correlation provides LFS values very close to those predicted by chemical kinetics, except for an equivalence ratio of 0.6, where the correlation slightly overpredicts the LFS values (Fig. 8 (a)) with the greatest deviation of approximately 11%. However, as the equivalence ratio increased beyond 0.6, the accuracy of the correlation also improved. This is attributable to the higher magnitudes of LFS associated with the equivalence ratio.

Fig. 9 shows that the LFS decreases linearly with increasing water addition for all pressures and temperatures, but the rate of decrease of the LFS of hydrogen was more pronounced at higher ambient temperatures of the reactive mixture. The correlation also reveals that the linear rate of decrease of LFS was evident even at lower ambient mixture temperatures of 400 K and equivalence ratio $\Phi = 1$ (Fig. 9(c and d)).

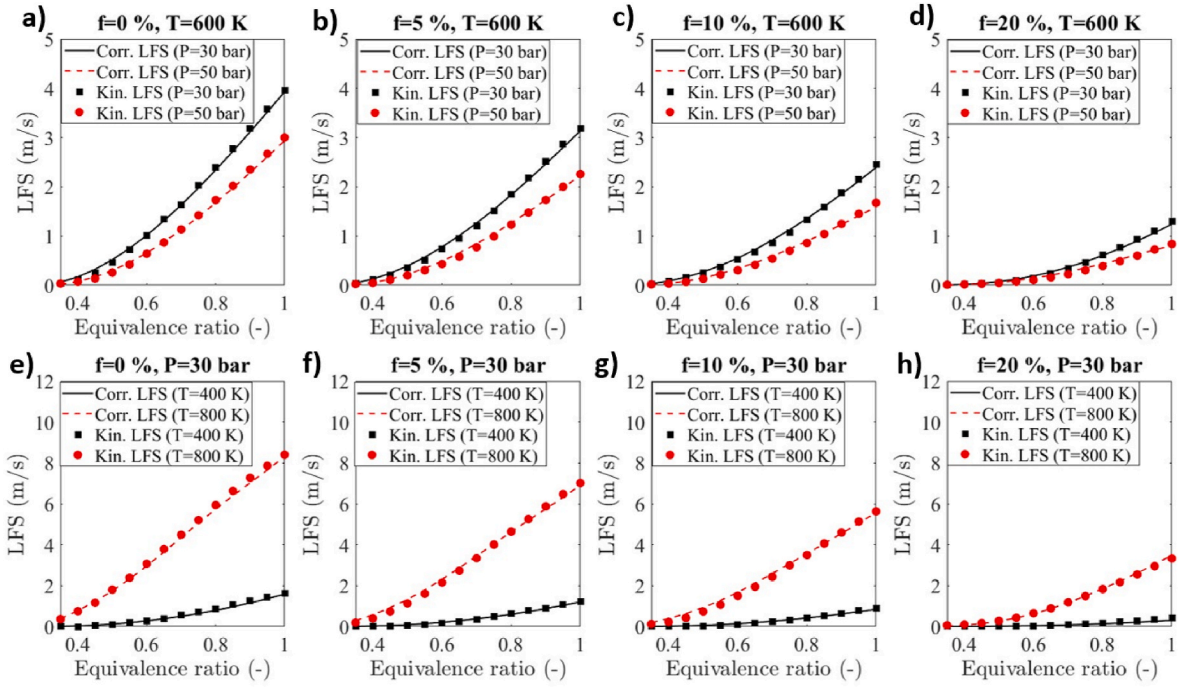

Fig. 7. Comparison of the chemical kinetic hydrogen laminar flame speed values with correlation values at various operating conditions.

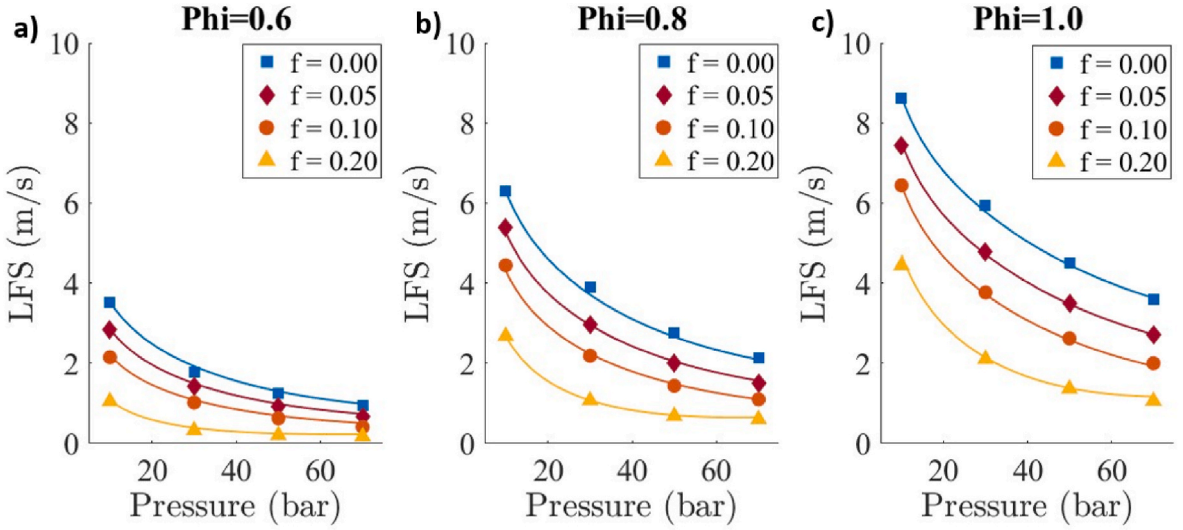

Fig. 8. Laminar flame speed values for various water additions (0–20%) at different pressures: (a) at equivalence ratio of 0.6; (b) at equivalence ratio of 0.8; and (c) at equivalence ratio of 1 at temperature of 700 K. Solid lines are correlation values and markers represent the chemical kinetic values.

However, the rate of decrease of flame speed was not that significant at $\Phi < 1$ at same lower ambient mixture temperatures of 400 K (Fig. 9 (a – b)). The correlation closely matches chemical kinetic LFS values, with exceptions at an equivalence ratio of 0.5 and pressures of 30 bar and 50 bar (Fig. 9(a and b)), respectively. Where the correlation slightly over-predicts the LFS values, the greatest deviation is approximately 13% (Fig. 9 (b)). However, as the equivalence ratio increases to the stoichiometric condition, the accuracy of the correlation improves for various temperatures, pressures, and water additions (Fig. 9(c and d)). The linear decrease in the rate of the LFS was noted with the addition of water, but there appears to be a limit to the amount of water addition for an effective control of hydrogen combustion beyond which it tends to be detrimental to the engine performance. This is due to a decrease in the global reaction temperature caused by the high heat capacity of the water vapour in the reactive mixture [39]. The LFS values increased with increasing temperature, a trend captured by the power, α, used in the correlation (Eq. (2)). As explained in subsection 2.2, α captures not only the effect of temperature but also the influence of the equivalence ratio and the coupled effect of pressure and temperature on the hydrogen LFS. The proposed correlation for hydrogen LFS with a reduced order of polynomial and reduced number of coefficients, shows that more than 97% of data are within the 20% accuracy level across various temperatures, pressures, equivalence ratios, and water addition conditions. The proposed correlation is sufficiently sensitive to predict variations of LFS under different conditions of pressure, temperature, equivalence and water additions. Error analysis of this correlation is discussed in next section.

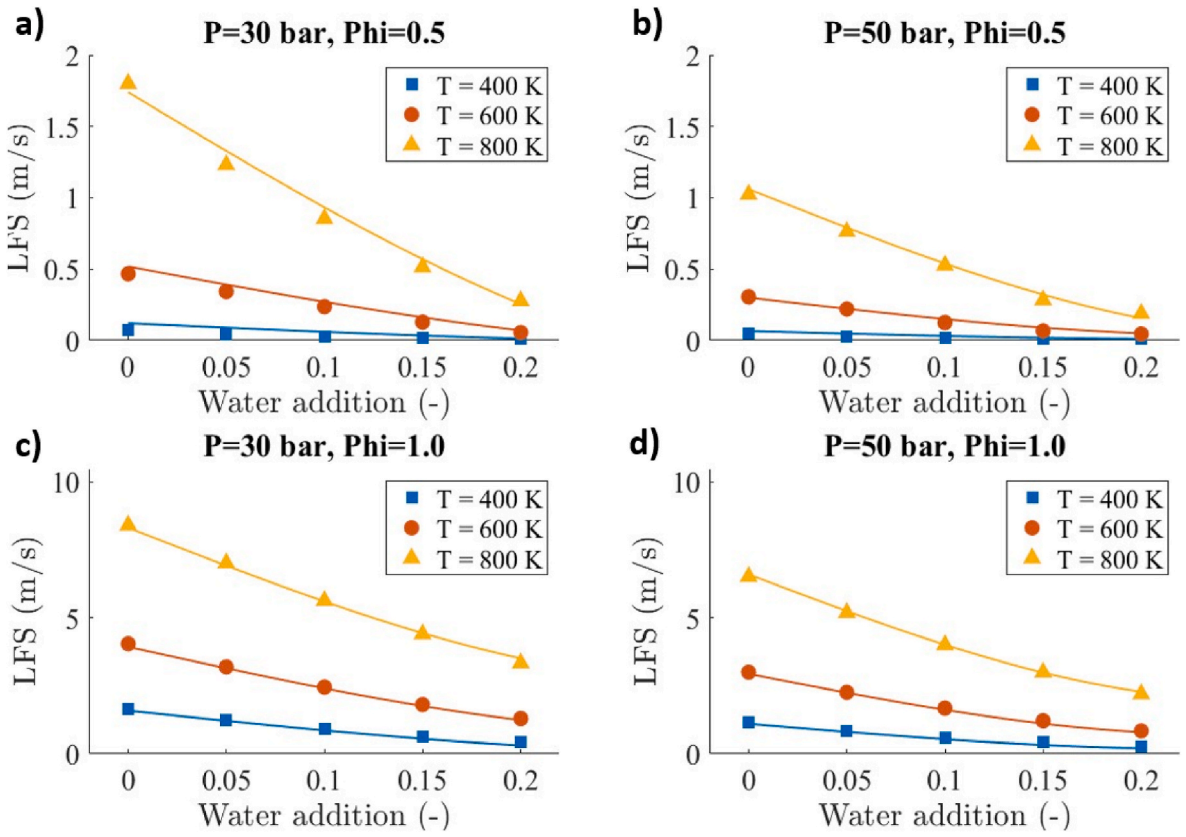

Fig. 9. Laminar flame speed values of hydrogen with various water additions at different temperatures, pressures, and equivalence ratios. Solid lines are correlation values and markers represent the chemical kinetic values.

3.3. Residual analysis

Fig. 10 (a) illustrates the hydrogen LFS error across a wide range of pressures from 10 to 70 bar, temperatures from 400 to 800 K, and equivalence ratios from 0.35 to 1. The accuracy of the pure hydrogen LFS values predicted from the proposed correlation is consistent with previous studies [6,7], as more than 99% of the data are within a 20% error margin. Furthermore, around 87% of the data were within a 10% deviation. To quantify the relative error, residuals between the chemical kinetics and the correlation flame speed values were calculated for selected operating conditions. The average mean error was within 5% for 5% and 10% water addition, within 4% for 15% water addition, and within 7% for 20% water addition. A comparison was also made between the hydrogen LFS values obtained from Eq. (4) with and without the term $exp\ (\beta T/T_0)$ and shown in Fig. 10 (b). It is evident that a significant number of data points had their residuals reduced significantly by incorporating the temperature-pressure coupling effect term into the hydrogen LFS correlation. Without the inclusion of this term in the α

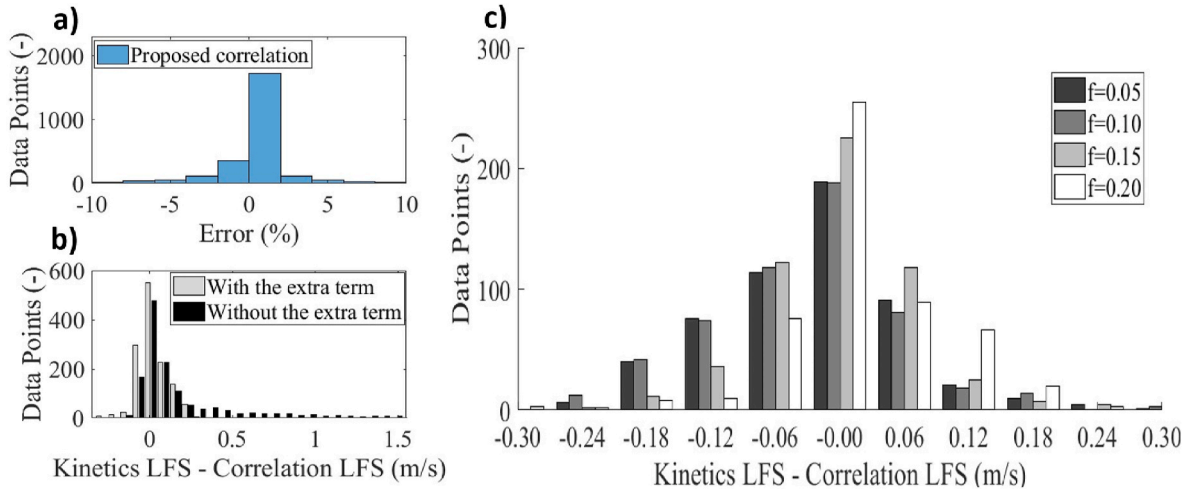

Fig. 10. (a) The standard error for the proposed hydrogen laminar flame speed correlation at various operating conditions (phi = 0.35–1, P = 10–70 bar and T = 400–800 K); (b) the histogram of the residuals for both of the equation with and without $\exp(\beta T/T_0)$ term; (c) the histogram of the residuals calculated as the difference between chemical kinetics and correlation laminar flame speed values (m/s) against the number of data points at different water addition (1–20%) and operating conditions (∅ = 0.35–1, P = 10–70 bar and T = 400–800 K).

calculation (Eq. (4)), the hydrogen LFS values would be underestimated, leading to residuals shifting to higher values. The addition of the temperature-pressure coupling term successfully refined the power α, minimizing the value of the residuals. These residuals were used to generate a histogram for various operating conditions of hydrogen with water addition (Fig. 10 (c)). The residuals were found to be unimodal, and the accuracy was assessed using the mean and standard deviation. It was observed that for each level of water addition, the histogram shape remained unimodal for all concentrations of water additions, with a peak at zero. The absolute values of mean residual were 0.1033, 0.1002, 0.0665, and 0.0887 m/s for 5%, 10%, 15%, and 20% water addition, respectively. When the molar fraction of water in the mixture increased, the residual magnitudes were reduced, correlating well with the decrease in hydrogen LFS values due to the water addition as shown in Figs. 8 and 9. Note that bars with less than 4 data points have not been included in Fig. 10(a–c).

4. Conclusion

The LFS is important for modelling internal combustion engines, but generating these from experiments or chemical kinetic simulations can be costly and time-consuming. Therefore, developing a correlation that can accurately predict the LFS under complex engine operating conditions is valuable. An empirical hydrogen LFS with water addition at engine-relevant operating conditions was developed in this study. The LFS correlation was validated for pressure ranges from 10 to 70 bar, temperature ranges from 400 to 800 K, equivalence ratio ranges from 0.35 to 1, and water addition by mole from 0 to 20%. The LFS of hydrogen-air mixtures, with and without water addition, were simulated using a chemical kinetic model [28]. Polynomial expressions of reduced order and number of terms were developed with optimized values of coefficients to predict the hydrogen LFS under lean mixture operation and high-pressure conditions. The variation between the simulated values from the chemical kinetic model and the predicted values from the proposed correlations of reduced order resulted in an R^2 value of 0.99. A new exponential term was proposed for the power term α in the correlation to capture the coupled effects of pressure, equivalence ratio, and temperature on LFS under engine-relevant lean burn, water-diluted operating conditions. This proposed correlation will help in bridging the knowledge gap for exploring the benefits of hydrogen-air combustion with water addition in engines, and in other power generators in the pursuit of zero carbon emissions.

Author contributions

D.N. Rrustemi: Formal analysis; Investigation; Methodology; Software; Validation; Visualization; Writing - original draft.

L.C. Ganippa: Methodology; Supervision; Writing - review.

T. Megaritis: Methodology; Writing - review.

C.J. Axon Conceptualization; Project administration; Supervision; Writing - review & editing.

Declaration of competing interest

The authors declare that they have no known competing financial interests or personal relationships that could have appeared to influence the work reported in this paper.

References

[1] Bae C, Kim J. Alternative fuels for internal combustion engines. Proc Combust Inst 2017;36:3389–413. https://doi.org/10.1016/j.proci.2016.09.009.

[2] Acar C, Dincer I. The potential role of hydrogen as a sustainable transportation fuel to combat global warming. Int J Hydrogen Energy 2020;45:3396–406. https://doi.org/10.1016/j.ijhydene.2018.10.149.

[3] Reitz RD, Ogawa H, Payri R, Fansler T, Kokjohn S, Moriyoshi Y, et al. IJER editorial: the future of the internal combustion engine. Int J Engine Res 2020;21:3–10. https://doi.org/10.1177/1468087419877990.

[4] Zaccardi J-M, Pilla G. Hydrogen as a combustion enhancer for highly efficient ultra-lean spark-ignition engines. 2019. p. 2019. https://doi.org/10.4271/2019-01-2258. 01–2258.

[5] Eckart S, Prieler R, Hochenauer C, Krause H. Application and comparison of multiple machine learning techniques for the calculation of laminar burning velocity for hydrogen-methane mixtures. Therm Sci Eng Prog 2022;32:101306. https://doi.org/10.1016/j.tsep.2022.101306.

[6] Verhelst S, T'Joen C, Vancoillie J, Demuynck J. A correlation for the laminar burning velocity for use in hydrogen spark ignition engine simulation. Int J Hydrogen Energy 2011;36:957–74. https://doi.org/10.1016/j.ijhydene.2010.10.020.

[7] Ravi S, Petersen EL. Laminar flame speed correlations for pure-hydrogen and high-hydrogen content syngas blends with various diluents. Int J Hydrogen Energy 2012;37:19177. https://doi.org/10.1016/j.ijhydene.2012.09.086. –89.

[8] Metghalchi M, Keck JC. Laminar burning velocity of propane-air mixtures at high temperature and pressure. Combust Flame 1980;38:143–54. https://doi.org/10.1016/0010-2180(80)90046-2.

[9] Konnov AA, Mohammad A, Kishore VR, Kim NI, Prathap C, Kumar S. A comprehensive review of measurements and data analysis of laminar burning velocities for various fuel+air mixtures. Prog Energy Combust Sci 2018;68:197–267. https://doi.org/10.1016/j.pecs.2018.05.003.

[10] Gerke U, Steurs K, Rebecchi P, Boulouchos K. Derivation of burning velocities of premixed hydrogen/air flames at engine-relevant conditions using a single-cylinder compression machine with optical access. Int J Hydrogen Energy 2010;35:2566–77. https://doi.org/10.1016/j.ijhydene.2009.12.064.

[11] Varghese RJ, Kolekar H, Kishore VR, Kumar S. Measurement of laminar burning velocities of methane-air mixtures simultaneously at elevated pressures and elevated temperatures. Fuel 2019;257:116120. https://doi.org/10.1016/j.fuel.2019.116120.

[12] Harbi A, Farooq A. Monte-Carlo based laminar flame speed correlation for gasoline. Combust Flame 2020;222:61–9. https://doi.org/10.1016/j.combustflame.2020.08.023.

[13] Del Pecchia M, Breda S, D'Adamo A, Fontanesi S, Irimescu A, Merola S. Development of chemistry-based laminar flame speed correlation for part-load SI conditions and validation in a GDI research engine. SAE Int J Engines 2018;11:715–41. https://doi.org/10.4271/2018-01-0174.

[14] D'Adamo A, Del Pecchia M, Breda S, Berni F, Fontanesi S, Prager J. Chemistry-based laminar flame speed correlations for a wide range of engine conditions for iso-octane, n-heptane, toluene and gasoline surrogate fuels. 2017. p. 2017. https://doi.org/10.4271/2017-01-2190. 01–2190.

[15] Üstün CE, Herfatmanesh MR, Valera-Medina A, Paykani A. Applying machine learning techniques to predict laminar burning velocity for ammonia/hydrogen/air mixtures. Energy and AI 2023;13:100270. https://doi.org/10.1016/j.egyai.2023.100270.

[16] Mehra RK, Duan H, Luo S, Ma F. Laminar burning velocity of hydrogen and carbon-monoxide enriched natural gas (HyCONG): an experimental and artificial neural network study. Fuel 2019;246:476–90. https://doi.org/10.1016/j.fuel.2019.03.003.

[17] Vom Lehn F, Cai L, Copa Cáceres B, Pitsch H. Exploring the fuel structure dependence of laminar burning velocity: a machine learning based group contribution approach. Combust Flame 2021;232:111525. https://doi.org/10.1016/j.combustflame.2021.111525.

[18] Wan Z, Wang Q-D, Wang B-Y, Liang J. Development of machine learning models for the prediction of laminar flame speeds of hydrocarbon and oxygenated fuels. Fuel Communications 2022;12:100071. https://doi.org/10.1016/j.jfueco.2022.100071.

[19] Rrustemi DN, Ganippa LC, Axon CJ. Investigation of boost pressure and spark timing on combustion and NO emissions under lean mixture operation in hydrogen engines. Fuel 2023;353:129192. https://doi.org/10.1016/j.fuel.2023.129192.

[20] Mortimer J, Poursadegh F, Brear M, Yoannidis S, Lacey J, Yang Y. Extending the knock limits of hydrogen DI ICE using water injection. Fuel 2023;335:126652. https://doi.org/10.1016/j.fuel.2022.126652.

[21] Xu P, Ji C, Wang S, Cong X, Ma Z, Tang C, et al. Effects of direct water injection on engine performance in engine fueled with hydrogen at varied excess air ratios and spark timing. Fuel 2020;269:117209. https://doi.org/10.1016/j.fuel.2020.117209.

[22] Duva BC, Toulson E. Unstretched unburned flame speed and burned gas Markstein length of diluted hydrogen/air mixtures. Int J Hydrogen Energy 2022;47:9030–44. https://doi.org/10.1016/j.ijhydene.2021.12.217.

[23] Meng S, Sun S, Xu H, Guo Y, Feng D, Zhao Y, et al. The effects of water addition on the laminar flame speeds of CO/H2/O2/H2O mixtures. Int J Hydrogen Energy 2016;41:10976–85. https://doi.org/10.1016/j.ijhydene.2016.04.251.

[24] Lipatnikov AN, Chomiak J. Molecular transport effects on turbulent flame propagation and structure. Prog Energy Combust Sci 2005;31:1–73. https://doi.org/10.1016/j.pecs.2004.07.001.

[25] Onorati A, Payri R, Vaglieco B, Agarwal A, Bae C, Bruneaux G, et al. The role of hydrogen for future internal combustion engines. Int J Engine Res 2022;23:529–40. https://doi.org/10.1177/14680874221081947.

[26] Verhelst S, Wallner T. Hydrogen-fueled internal combustion engines. Prog Energy Combust Sci 2009;35:490–527. https://doi.org/10.1016/j.pecs.2009.08.001.

[27] Richards KJ, Senecal PK, Pomraning E. Converge 3.0. Madison, WI: Convergent Science; 2023. www.convergentcfd.com. [Accessed 18 March 2024].

[28] Li J, Zhao Z, Kazakov A, Dryer FL. An updated comprehensive kinetic model of hydrogen combustion. Int J Chem Kinet 2004;36:566–75. https://doi.org/10.1002/kin.20026.
[29] Iijima T, Takeno T. Effects of temperature and pressure on burning velocity. Combust Flame 1986;65:35–43. https://doi.org/10.1016/0010-2180(86)90070-2.
[30] Koroll G, Kumar R, Bowles E. Burning velocities of hydrogen-air mixtures. Combust Flame 1993;94:330–40. https://doi.org/10.1016/0010-2180(93)90078-H.
[31] Verhelst S, Woolley R, Lawes M, Sierens R. Laminar and unstable burning velocities and Markstein lengths of hydrogen–air mixtures at engine-like conditions. Proc Combust Inst 2005;30:209–16. https://doi.org/10.1016/j.proci.2004.07.042.
[32] Kwon OC, Faeth GM. Flame/stretch interactions of premixed hydrogen-fueled flames: measurements and predictions. Combust Flame 2001;124:590–610. https://doi.org/10.1016/S0010-2180(00)00229-7.
[33] Koroll GW, Mulpuru SR. The effect of dilution with steam on the burning velocity and structure of premixed hydrogen flames. Symposium (International) on Combustion 1988;21:1811–9. https://doi.org/10.1016/S0082-0784(88)80415-6.
[34] Lyu Y, Qiu P, Liu L, Yang C, Sun S. Effects of steam dilution on laminar flame speeds of H2/air/H2O mixtures at atmospheric and elevated pressures. Int J Hydrogen Energy 2018;43:7538–49. https://doi.org/10.1016/j.ijhydene.2018.02.065.
[35] Cavanaugh JE, Neath AA. The Akaike information criterion: background, derivation, properties, application, interpretation, and refinements. WIREs Computational Stats 2019;11:e1460. https://doi.org/10.1002/wics.1460.
[36] Kuznetsov M, Redlinger R, Breitung W, Grune J, Friedrich A, Ichikawa N. Laminar burning velocities of hydrogen-oxygen-steam mixtures at elevated temperatures and pressures. Proc Combust Inst 2011;33:895–903. https://doi.org/10.1016/j.proci.2010.06.050.
[37] Zhang W, Gou X, Kong W, Chen Z. Laminar flame speeds of lean high-hydrogen syngas at normal and elevated pressures. Fuel 2016;181:958–63. https://doi.org/10.1016/j.fuel.2016.05.013.
[38] Eisazadeh-Far K, Moghaddas A, Metghalchi H, Keck JC. The effect of diluent on flame structure and laminar burning speeds of JP-8/oxidizer/diluent premixed flames. Fuel 2011;90:1476–86. https://doi.org/10.1016/j.fuel.2010.11.020.
[39] Law CK. Combustion physics. first ed. Cambridge University Press; 2006. https://doi.org/10.1017/CBO9780511754517.